

Full-scale investigations into installation damage of nonwoven geotextiles

Ehsan Amjadi Sardehaei¹, Gholamhossein Tavakoli Mehrjardi^{2,*} and Andrew Dawson³

¹ Post-graduated, Department of Civil Engineering, Faculty of Engineering, Kharazmi University, Tehran, Iran

² Assistant Professor, Department of Civil Engineering, Faculty of Engineering, Kharazmi University, Tehran, Iran

³ Associate Professor, Nottingham Transportation Engineering Centre, University of Nottingham, Nottingham, UK

Abstract. Due to the importance of soil reinforcement using geotextiles in geotechnical engineering, study and investigation into long-term performance, design life and survivability of geotextiles, especially due to installation damage are necessary and will affect their economy. During installation, spreading and compaction of backfill materials, geotextiles may encounter severe stresses which can be higher than they will experience in-service. This paper aims to investigate the installation damage of geotextiles, in order to obtain a good approach to the estimation of the material's strength reduction factor. A series of full-scale tests were conducted to simulate the installation process. The study includes four deliberately poorly-graded backfill materials, two kinds of subgrades with different CBR values, three nonwoven needle-punched geotextiles of classes 1, 2 and 3 (according to AASHTO M288-08) and two different relative densities for the backfill materials. Also, to determine how well or how poorly the geotextiles tolerated the imposed construction stresses, grab tensile tests and visual inspections were carried out on geotextile specimens (before and after installation). Visual inspections of the geotextiles revealed sedimentation of fine-grained particles in all specimens and local stretching of geotextiles by larger soil particles which exerted some damage. A regression model is proposed to reliably predict the installation damage reduction factor. The results, obtained by grab tensile tests and via the proposed models, indicated that the strength reduction factor due to installation damage was reduced as the median grain size and relative density of the backfill decreases, stress transferred to the geotextiles' level decreases and as the as-received grab tensile strength of geotextile and the subgrades' CBR value increase.

Keywords: geotextiles; installation damage; grab tensile strength; retained tensile strength; strength reduction factor.

1. Introduction

*Corresponding author, E-mail: ghtavakoli@khu.ac.ir

45
46 The advent of oil industries and polymer sciences resulted in the development of geotextiles to
47 solve some technical problems in civil engineering. They have been extensively applied in soil
48 reinforcement of geotechnical projects such as embankments over soft subgrades, road
49 construction, slopes, retaining walls and buried pipelines (Wang et al. 2011, Tavakoli
50 Mehrjardi et al. 2013, Naeini and Gholampoor 2014, Portelinha et al. 2013 and 2014, Tandel et
51 al. 2014, Deb and Konai, 2014, Hosseinpour et al. 2015, Viera et al. 2015, Kim et al. 2015,
52 Costa et al. 2016).

53 Geotextiles can potentially lose some of their original tensile strength due to various
54 destructive impacts such as the stresses exerted during installation, due to creep and from
55 environmental conditions. For instance, Vieira and Pereira (2015) studied the chemical and
56 environmental degradation induced by a recycled construction and demolition waste on the
57 short-term tensile behavior of two geosynthetics (a uniaxial HDPE geogrid and a nonwoven PP
58 geotextile reinforced with PET yarns). As expected the degradation induced by the recycled
59 construction and demolition waste after 6 months of exposure was not very expressive. The
60 primary reduction factor applied to the tensile strength of the geotextiles is due to installation
61 damage. In fact, during the installation process, geotextiles may encounter more stresses than
62 during their service life, with the appearance of cuts, frays and general abrasion. Koerner and
63 Koerner (1990) exhumed 75 different geotextiles and geogrids from 48 construction sites and
64 assessed the retained tensile strength after installation and excavation. The results revealed
65 that coarse, irregular and frozen subgrades, poorly graded cover soil with large particles,
66 small lift thicknesses and heavy construction equipment created severe damage. Furthermore,
67 Allen and Bathurst (1994) summarized the results of tensile load-strain tests performed on
68 different geosynthetic reinforcement products in site-damaged and undamaged conditions.
69 They observed greater loss of modulus for nonwoven geotextiles compared with woven
70 geotextiles and geogrids, owing to the thinner fibers employed by nonwoven geotextiles.
71 Greenwood and Brady (1992) and Richardson (1998) showed that the reduction factor due to
72 installation damage and the frequency of damage increased when increasing the backfill grain
73 size and number of passes.

74 Bathurst et al (2011) analyzed a database of results from field installation damage trials on
75 103 different geosynthetic products. This database had been collected from 20 different sources
76 for Load and Resistance Factor Design (LRFD) calibration of reinforced soil structures. In this
77 study, the formulation of the limit state for reinforcement tensile rupture is developed and the
78 component strength-reduction bias statistics identified. Installation damage bias statistics were
79 reported for six different categories of geosynthetic and four categories of backfill soils
80 classified according to the D_{50} particle size. They showed how bias statistics together with load
81 and resistance factors for the geosynthetic rupture limit state function can be used to calculate
82 the probability of failure using Monte Carlo simulation and demonstrated the sensitivity of
83 probability of failure to the magnitude of the installation damage bias statistics.

84 Most researchers emphasize that the level of damage depends directly on the weight, type
85 and number of passes of the compaction equipment. On the other hand, compaction of the
86 backfill by a lighter compactor tends to reduce the installation damage of the geotextiles (Watts
87 and Brady 1994, Watn et al. 1998, Elvidge and Rymond 1999, Pinho-Lopes and Lopes 2013,
88 Hufenus et al. 2005). Hufenus et al. (2005) found out that the survivability of geosynthetics
89 (specifically geogrids and geotextiles) primarily depends on the type of geosynthetic (fabric
90 design, type of tensile element) and, secondarily, on the nature of the polymer. The installation

91 damage of individual geotextiles is predominantly influenced by the size distribution and
92 geometry of the soil particles as well as the compaction energy. Nikbakht and Diederich (2008)
93 used the area under the stress-strain curve in wide-width tensile tests as an indication of the
94 energy absorption abilities of geotextiles. They showed that the retained strength increased and
95 strength reduction factor decreased with increasing ability to absorb energy.

96 AASHTO M288-08 categorizes three different classes for geotextiles (1, 2 and 3) based on
97 their survivability, according to the geotextiles' application and their physical and mechanical
98 properties. Class 1 is specified for more severe or harsh installation conditions where there is a
99 greater potential for geotextile damage while Classes 2 and 3 are specified for less severe
100 conditions (Watn et al. 1998, Richardson 1998, Elvidge and Rymond 1999, Nikbakht and
101 Diederich 2008, Rosete et al. 2013, Pinho-Lopes and Lopes 2013, Carlos et al. 2015). Richardson
102 (1998) clarified that installation damage to geotextiles can be minimized by applying at least 15cm
103 initial lift of fill over the geotextiles prior to compaction and a maximum stone size in the initial
104 lift to less than $\frac{1}{4}$ of the lift thickness. In such a situation, a minimum survivability "Class 2"
105 geotextile would be needed (although Class 1 is preferable).

106 FHWA-NHI-00-044 presented installation damage reduction factors for different types of
107 geotextiles, depending on the backfill soil grading. This guideline states that, in the absence of
108 project specific data, the largest indicated reduction factors should be used.

109 Although, there have been many studies into the installation damage of geotextiles, yet there is
110 a lack of investigation into the response of geotextiles after installation with respect to a suite of
111 different parameters such as aggregate size, subgrade stiffness, relative density of the backfill and
112 class of geotextile. Therefore, the specific aims of this study are:

- 113 • To investigate geotextile damage by use of a series of full-scale field tests,
- 114 • To investigate and to compare effects of the above-mentioned parameters on the installation
115 damage reduction factor of geotextiles,
- 116 • To formulate the relation between reduction factors owing to installation damage and the afore-
117 mentioned parameters,
- 118 • To correlate the installation damage reduction factor of geotextiles to these factors,
- 119 • To gain understanding of the caused damage by visual inspection of the geotextiles, before and
120 after installation.

121 The study has been performed on full-scale field installations and should give responses that
122 are broadly similar to those that which would be expected in normal practice.

124 **2. Test materials**

126 *2.1 Backfill materials*

128 In contrast with most experimental studies which investigate combinations of geotextiles and
129 well-graded soils, this study, in order to have better accuracy and assessment of the effect of
130 particle size, used poorly-graded backfill. These kinds of backfill are more common when a
131 geotextile's reinforcement application involves ballast or backfill behind the retaining walls. Thus,
132 four types of uniformly graded (poorly-graded) soils were used as backfill materials with the
133 median grain size (D_{50}) of 3, 6, 12 and 16 mm. The properties of these backfill materials, which
134 are classified as SP and GP in the unified Soil classification System, are summarized in Table 1.
135 Also, the grading of backfill materials is graphically illustrated in Fig. 1.

136

137
138
139
140
141
142
143
144
145
146

2.2 Subgrade

Two types of well-graded course materials namely “fine-grained subgrade, FS” and “coarse-grained subgrade, CS” were used to simulate the subgrade. The properties of these soils are presented in Table 2. In this study, “FS” and “CS” are intended to provide soft and stiff bases for geotextiles, respectively. The grading of the subgrades is presented graphically in Fig. 2.

Table 1 Physical properties of backfill materials

Description	Sand 3 mm	Gravel 6 mm	Gravel 12 mm	Gravel 16 mm
Coefficient of uniformity, C_u	2.125	2.14	1.33	1.27
Coefficient of curvature, C_c	1.19	1.08	0.95	0.96
Effective grain size, D_{10} (mm)	1.52	2.92	9.75	13.6
D_{30} (mm)	2.42	4.43	11	15
Median grain size, D_{50} (mm)	3.1	5.9	12.5	16.5
D_{60} (mm)	3.23	6.24	13	17.3
Specific gravity, G_s	2.419	2.494	2.546	2.604
Moisture content (%)	Dry	Dry	Dry	Dry
Percentage of fractured particles* (%)	85	80	83	82
Classification (USCS)	SP	GP	GP	GP

*The percentage of soil grains by weight in which the particles are not completely spherical and round. This was determined according to the ASTM D 5821-13.

147
148
149

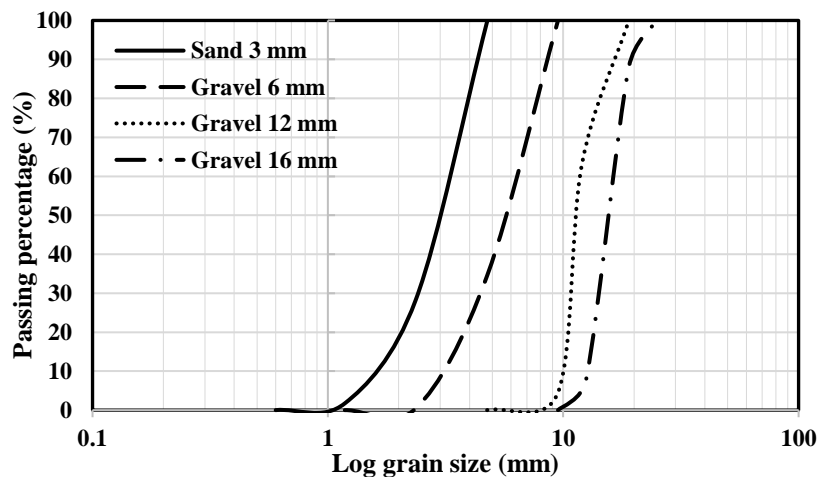


Fig. 1 Grain size distribution curves for backfill materials

150

Table 2 Physical properties of subgrades

Description	CS	FS
Coefficient of uniformity, C_u	10.95	7.16
Coefficient of curvature, C_c	2.86	1.55
Effective grain size, D_{10} (mm)	0.42	0.183
D_{30} (mm)	2.35	0.61
Median grain size, D_{50} (mm)	3.65	1.00
D_{60} (mm)	4.6	1.31
CBR soaked (%)	49	27
Moisture content (%)	5	5
Maximum dry unit weight, $\gamma_{d(max)}$ (kN/m ³)	19.36	17.18
Classification (USCS)	SW	SW

151

152

153

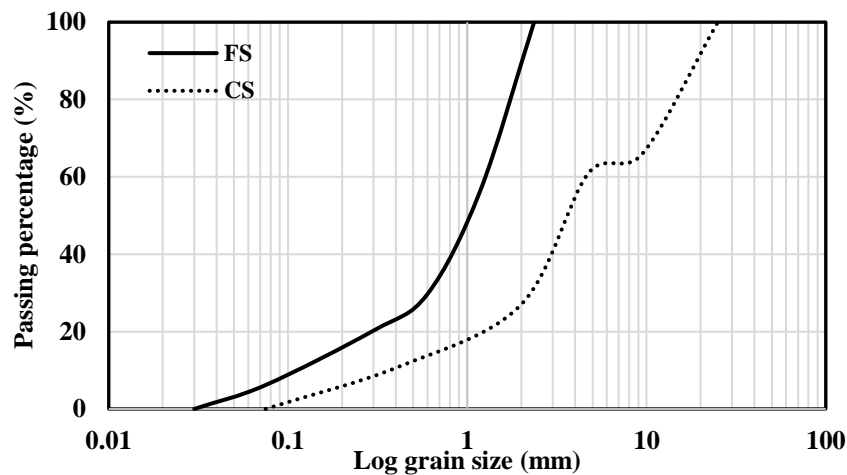


Fig. 2 Grain size distribution curves for subgrades

154

155

156

157

2.3 Geotextiles

158

159

160

161

162

Three types of needle-punched nonwoven geotextiles, made of polypropylene, are used, representing Classes 1, 2 and 3 in accordance with AASHTO M 288-08. The engineering properties of the geotextiles are provided in Table 3 (ASTM D 4533-15, D 4632-15a, D 5261-14, D 6241-10).

163
164
165

Table 3 Engineering properties of the geotextiles used

Description	Test methods	GT ₃	GT ₂	GT ₁
Mass per unit area (g/m ²)	ASTM D 5261-10	292	319	508
Grab tensile strength (N)	ASTM D 4632-15a	650	800	1350
Grab elongation (%)	ASTM D 4632-15a	> 50	> 50	> 50
Trapezoidal tear strength (N)	ASTM D 4533-15	310	385	600
CBR puncture (N)	ASTM D 6241-14	900	1500	2500
Class	AASHTO M 288-08	3	2	1

166
167
168
169
170
171

3. Testing Methods

3.1 Full-scale field model tests

172
173
174
175
176
177
178
179
180
181

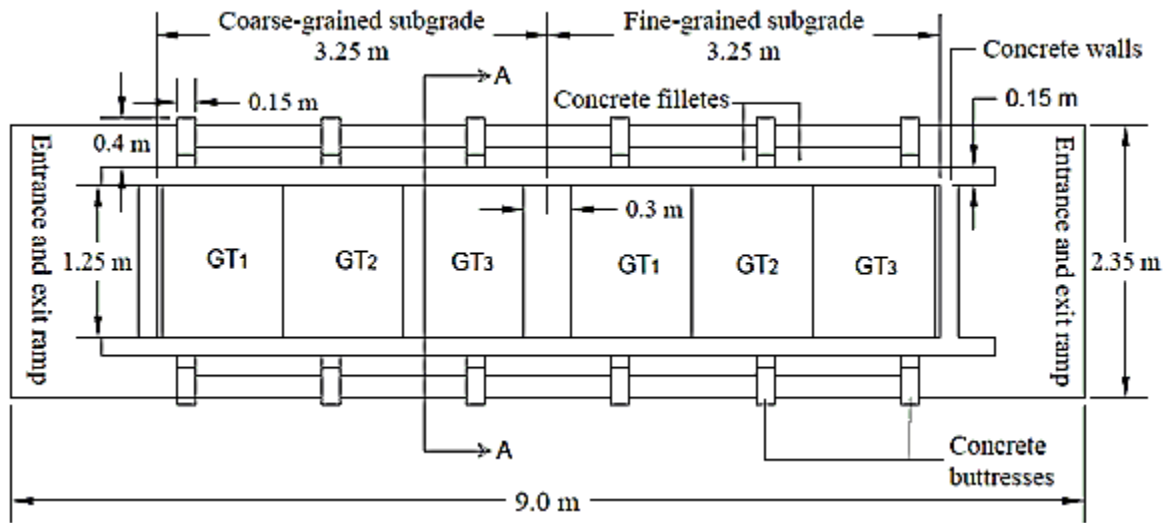
In order to simulate the installation process of geotextiles in unpaved roads, a physical model was developed by the authors. Fig. 3 shows the schematic representation of the test setup. The test area was divided by the two kinds of subgrades (“FS”:soft and “CS”:stiff). Prior to the subgrades’ construction, all obstacles such as trees root, grass, meadow mat and vegetative soil cover were removed. The subgrades were constructed and compacted with plane surfaces using a walk-behind tandem vibratory roller in a layer of 150mm-lift thickness, having 5% water content to achieve a relative density of at least 95%. As can be seen in Fig. 3(a), six tests can be set up in each round of installations. The test zones were surrounded by concrete frame supported by buttresses, having thickness and depth of 150 mm, to prevent spreading of the backfill during the compaction process (Fig. 3 (b)).

182
183
184
185
186
187
188
189
190
191

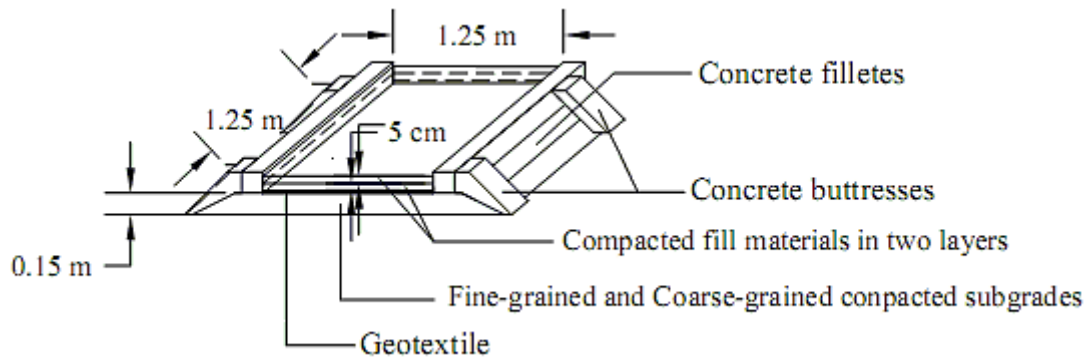
In all installations the subgrades were next covered by geotextiles (of Classes 1, 2 or 3), each being 1000 mm × 1200 mm in plan. Then, one of the backfill materials was placed into the frame above the geotextiles over the full length of the test area (see Fig. 4). The backfill was placed in two layers, each of 50mm-lift thickness. In order to compact the backfill, the same walk-behind tandem roller was used, but this time without vibration, to achieve the desired relative density ($D_r \approx 70\% = C1$ (medium dense) and $D_r \approx 90\% = C2$ (very dense), using 8 and 10 roller passes, respectively) of the soils. Details of the compactor specifications are presented in Table 4. To have a better assessment of the backfill and subgrade compaction, in some installations and after backfill placement, soil densities were measured according to ASTM D1556-07.

192
193
194
195
196

At the end of the compaction process, the backfill was carefully removed to ensure that the geotextiles could be exhumed without any additional damage. Then, visual inspections and grab tensile tests, as described in the following Sections (3.2 and 3.3), were performed on the exhumed samples of geotextiles (Tavakoli Mehrjardi and Amjadi 2017).



(a)



(b)

Fig. 3 Schematic representation of the test setup (a) plan (b) section A-A

197



(a)



(b)

Fig. 4 Photos of full-scale field tests (a) geotextile installation (b) backfill compaction

198
199

Table 4 The detail of walk-behind tandem vibratory roller

Total width (mm)	Diameter/Width of wheels (mm)	Total mass (kg)	Mass/unit area (kg/cm ²)	Speed of forward and reverse (km/h)
895	480/750	950	1.27	0-1.6

200
201
202
203

3.2 Visual inspection

204
205
206
207
208

In order to inspect the installation damage caused to the geotextiles, all of the samples were first inspected by eye. To have a better visual assessment, samples of geotextiles both before and after installation, were scanned and some image processing was performed to estimate degradation in the texture of the geotextiles. The observations are reported in Section 5.1.

209
210

3.3 Grab tensile strength test

211
212
213
214
215
216
217
218
219
220
221
222
223
224
225
226
227
228

AASHTO M288-08 classifies geotextile as 1, 2 or 3 based on strength property. The grab tensile strength (ASTM D 4632-15) is used to assess the geotextile's mechanical strength under direct tension. In order to quantify the damage severity of the geotextiles, following installation, grab tensile strengths of the exhumed geotextiles were assessed and compared to the strengths obtained from specimens which had never been installed beneath the backfill. Specimens of geotextiles with dimensions of 203.2 mm × 101.6 mm were punched from the parent material. Sampling was performed according to ASTM D5818-00. Then, having placed the specimens in the test machine with a free distance of 75 mm between the clamps, the tensile testing machine applied tensile loading at a rate of 300 mm/minute till rupture takes place. During the test, grab tensile forces are accompanied by corresponding elongations which are, simultaneously, recorded. The grab tensile test was carried out on three specimens in each case and the representative mean result has been reported as retained grab tensile strength in Tables 3 and 7. The number of tests on damaged and undamaged samples (3 each) did not comply with North American practice for product certification. The WSDOT T925 (2005) installation damage test protocol calls for a minimum of five undamaged specimens and nine or more damaged specimens depending on the COV of strength values for the exhumed (damaged) specimens (Bathurst et al., 2011).

229
230

4. Test programme

231
232
233
234
235
236

Table 5 gives details of the test series performed in this study. For easy recognition, a system of test coding was defined (Table 6). Each test is coded in the form A-B-C-D, where "A" signifies the class of geotextile, "B" the subgrade type, "C" the backfill material and "D" the relative density of the backfill. For example, the test with the code GT1-CS-6-C1, has a geotextile of Class 1 installed on coarse-grained subgrade covered by backfill with $D_{50}=6$ mm and compacted with $D_r=70\%$.

237 Table 5 Testing Programme

Geotextiles' Class	Subgrades' CBR (%)	Relative Density (%)	Median Grain Size (mm)	No. of Tests
1	27 and 49	70 and 90	3, 6, 12 and 16	16
2	27 and 49	70 and 90	3, 6, 12 and 16	16
3	27 and 49	70 and 90	3, 6, 12 and 16	16

238

239

240

Table 6 Symbol of variable parameters for coding the geotextile specimens

Geotextile type	Symbol	Subgrade type	Symbol	Backfill type	Symbol	Relative density of backfill materials	Symbol
Class 1	GT ₁	Coarse-grained	CS	Sand 3 mm	3	70 %	C ₁
Class 2	GT ₂	Fine-grained	FS	Gravel 6 mm	6	90 %	C ₂
Class 3	GT ₃			Gravel 12 mm	12		
				Gravel 16 mm	16		

241

242

5. Results and Discussions

243

244

5.1 Visual inspection

245

246

247

Among the possible types of damage that can be caused by installation, the following outcomes were investigated: cutting, fraying, very fine-grained particles pushed into the texture, fiber separation, holes and local stretching of geotextiles by larger soil particles.

248

249

250

251

252

253

254

255

256

According to the visual inspections, there was no fraying, fiber separation nor holes. However, in all specimens, fine-grained particles with a size of about 0 to 2 mm penetrated into the texture of the geotextiles. Although, the aggregates did not puncture the geotextiles, backfills with larger particles, especially with a median grain size of 12 and 16 mm, squeezed into the texture, specifically in Class 2 and Class 3 geotextiles. An explanation may be that increasing the grain size will decrease the number of stone-stone contacts but each having a higher contact force and that, therefore, this tends to transfer more stress onto the geotextiles. As expected, geotextile Class 1, due to its greater thickness, appeared to be less damaged by the installation process than others.

257

5.2 Grab tensile test

258

259

260

261

262

263

264

As Table 7 compares the values of grab tensile strength obtained before and after installation. It might be expected that the retained tensile strength of the geotextiles (T_{ID}) should be less than the as-received tensile strength (T_0); but, as can be seen in Table 7, 14 tests out of 48 tests have retained tensile strengths more than their original strengths (for most of them, just a little larger than their original strength). This may have happened because of non-uniformity in the texture of geotextiles, resulting in strengths varying with position in the geotextiles sheet. Another cause may be due to local strain-hardening caused by fiber distortion. This matter has been observed by some

265 previous researchers (Greenwood and Brady 1992, Allen and Bathurst 1994, Hufenus et al. 2005).
 266 Allen and Bathurst (1994) stated that this effect may be due to the accumulation of fine particles in
 267 the fiber matrix of geotextiles and, possibly, the result of “strain hardening” of polyolefin materials
 268 due to locked-in tensile load during compaction.

269
 270
 271

Table 7 Values of retained grab tensile strength obtained after exhumation for each test condition

Test code	Tensile strength (N)	Test code	Tensile strength (N)	Test code	Tensile strength (N)
GT ₁ -CS-3-C ₁	1321	GT ₂ -FS-6-C ₁	666	GT ₃ -CS-12-C ₂	575
GT ₂ -CS-3-C ₁	893	GT ₃ -FS-6-C ₁	690	GT ₁ -FS-12-C ₂	1206
GT ₃ -CS-3-C ₁	599	GT ₁ -CS-6-C ₂	1243	GT ₂ -FS-12-C ₂	695
GT ₁ -FS-3-C ₁	1397	GT ₂ -CS-6-C ₂	662	GT ₃ -FS-12-C ₂	704
GT ₂ -FS-3-C ₁	743	GT ₃ -CS-6-C ₂	605	GT ₁ -CS-16-C ₁	1459
GT ₃ -FS-3-C ₁	633	GT ₁ -FS-6-C ₂	1325	GT ₂ -CS-16-C ₁	920
GT ₁ -CS-3-C ₂	1332	GT ₂ -FS-6-C ₂	659	GT ₃ -CS-16-C ₁	604
GT ₂ -CS-3-C ₂	887	GT ₃ -FS-6-C ₂	615	GT ₁ -FS-16-C ₁	1222
GT ₃ -CS-3-C ₂	676	GT ₁ -CS-12-C ₁	1333	GT ₂ -FS-16-C ₁	704
GT ₁ -FS-3-C ₂	1289	GT ₂ -CS-12-C ₁	848	GT ₃ -FS-16-C ₁	538
GT ₂ -FS-3-C ₂	755	GT ₃ -CS-12-C ₁	599	GT ₁ -CS-16-C ₂	1286
GT ₃ -FS-3-C ₂	644	GT ₁ -FS-12-C ₁	1387	GT ₂ -CS-16-C ₂	597
GT ₁ -CS-6-C ₁	1283	GT ₂ -FS-12-C ₁	725	GT ₃ -CS-16-C ₂	578
GT ₂ -CS-6-C ₁	731	GT ₃ -FS-12-C ₁	658	GT ₁ -FS-16-C ₂	1416
GT ₃ -CS-6-C ₁	632	GT ₁ -CS-12-C ₂	1375	GT ₂ -FS-16-C ₂	823
GT ₁ -FS-6-C ₁	1237	GT ₂ -CS-12-C ₂	750	GT ₃ -FS-16-C ₂	634

272
 273
 274
 275
 276
 277
 278

Figs. 5 to 9 are presented to study the effects of median grain size of backfill materials, the relative density of backfill materials, the geotextiles class and the type of subgrades on the retained tensile strength of the geotextiles. In some of these figures (Figs. 5 and 6) a trend line for either all results, named “48-test”, or for results where the retained tensile strengths were smaller than the as-received tensile strength, named “34-test”, is illustrated. As can be seen in Figs. 5 and 6,

279 according to the “48-test results”, tensile strengths of the geotextiles have mostly decreased with
280 increase of median grain size of the backfill. As explained in the earlier section (5.1) on visual
281 inspection, increasing the grain size tends to transfer more stress onto the geotextiles, leading to a
282 reduction in the ultimate tensile strength.

283 From Fig. 7 shows that tensile strengths of the geotextile were mostly decreased following
284 compaction of the backfill to the higher relative density. This is probably because the higher
285 relative density, obtained by an increased mass of backfill over the geotextile in addition to the
286 increased number of compactor passes, resulted in transfer of more energy on geotextile and
287 thereby, reduction in the retained tensile strength. These results are in line with the findings of
288 previous investigators (Greenwood and Brady 1992, Richardson 1998, Elvidge and Raymond
289 1999, Elias 2001, Mendes et al. 2007, Pinho-Lopes and Lopes 2013, Carlos et al. 2015).

290 Mechanical properties of the geotextiles are another parameter which significantly affects the
291 installation damage. According to Fig. 8, it can be seen that by increasing the tensile strength of
292 the geotextiles (changing the geotextiles class from 3 to 1), the survivability would be increased.
293 As a rule-of-thumb, it is obvious that the minimum reduction factor (the ratio of as-received tensile
294 strength to retained tensile strength of the geotextiles) equals 1.11, and belongs to geotextile Class
295 1 (Want et al. 1998, Richardson 1998, Elvidge and Raymond 1999, Nikbakht and Diederich 2008,
296 Pinho-Lopes and Lopes 2013, Rosete et al. 2013, Carlos et al. 2015).

297 According to majority of the results shown in Fig. 9, the subgrade stiffness had a positive
298 influence on the survivability of the geotextiles. It seems that reduction in the CBR value of the
299 subgrade allowed movement beneath the geotextile, leading to more tension in the geotextile and,
300 thereby, causing greater damage.

301 It should be mentioned that the impacts of relative density of the backfill and subgrade type on
302 installation damage of the geotextiles were accompanied with some uncertainty and scatter.
303 Perhaps, for this reason, FHWA-NHI-10-024 focuses on the grain size of backfill and geotextile
304 type to suggest reduction factors due to installation damage.

305 Given that damage is widespread, even if not always discovered, the “34-test” results provide a
306 more conservative assessment of damage. Therefore, the study continues based only on the “34-
307 test” results.

308
309
310
311
312
313
314

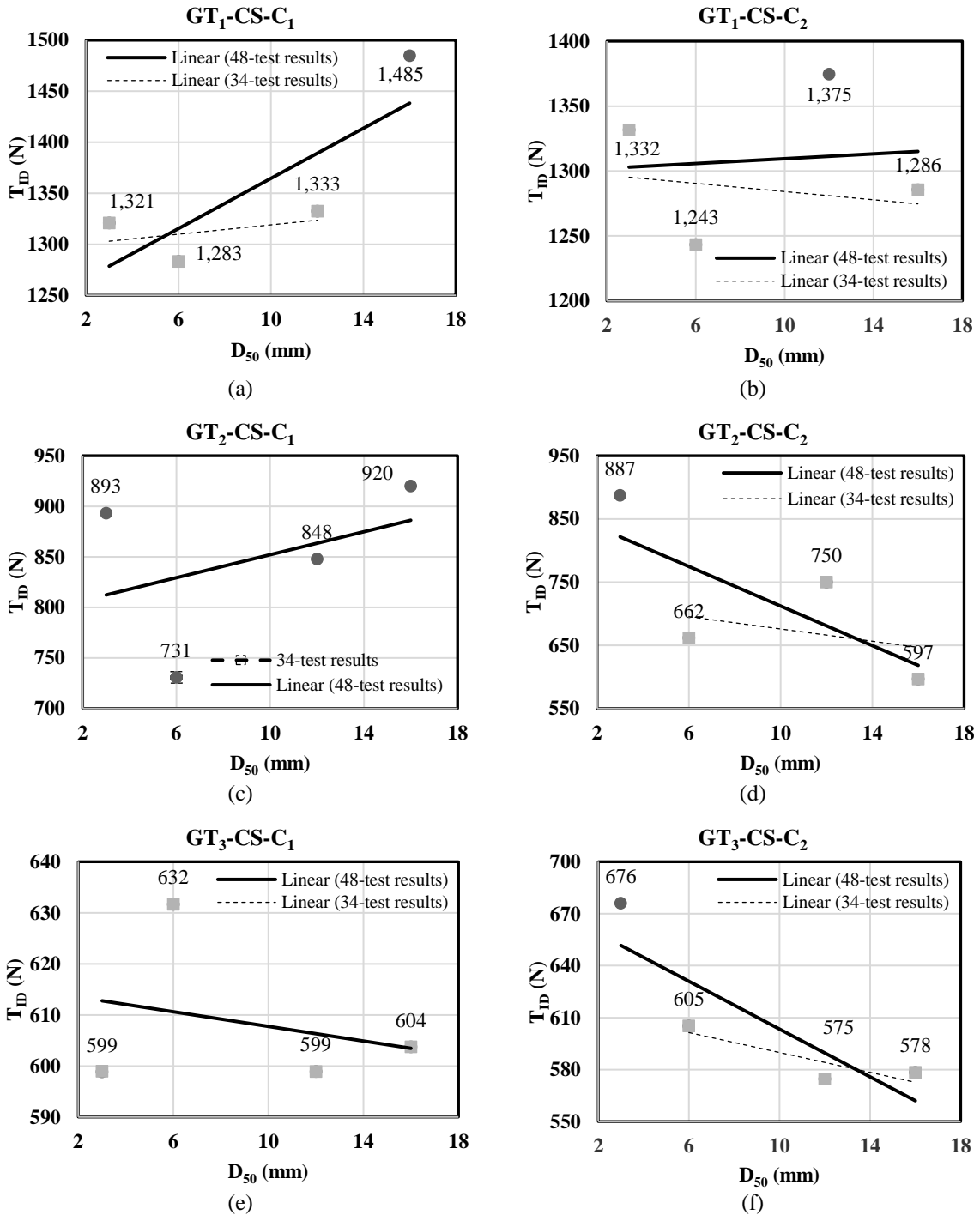


Fig. 5 Retained geotextile tensile strengths for different size backfills all on subgrade “CS”. $Dr=70\%$ for (a), (c) & (e), $Dr=90\%$ for (b), (d) & (f). Solid lines and dashed lines are plotted with and without considering the “circle points”, respectively. These “circle points” represent retained tensile strengths larger than the as-received tensile strengths.

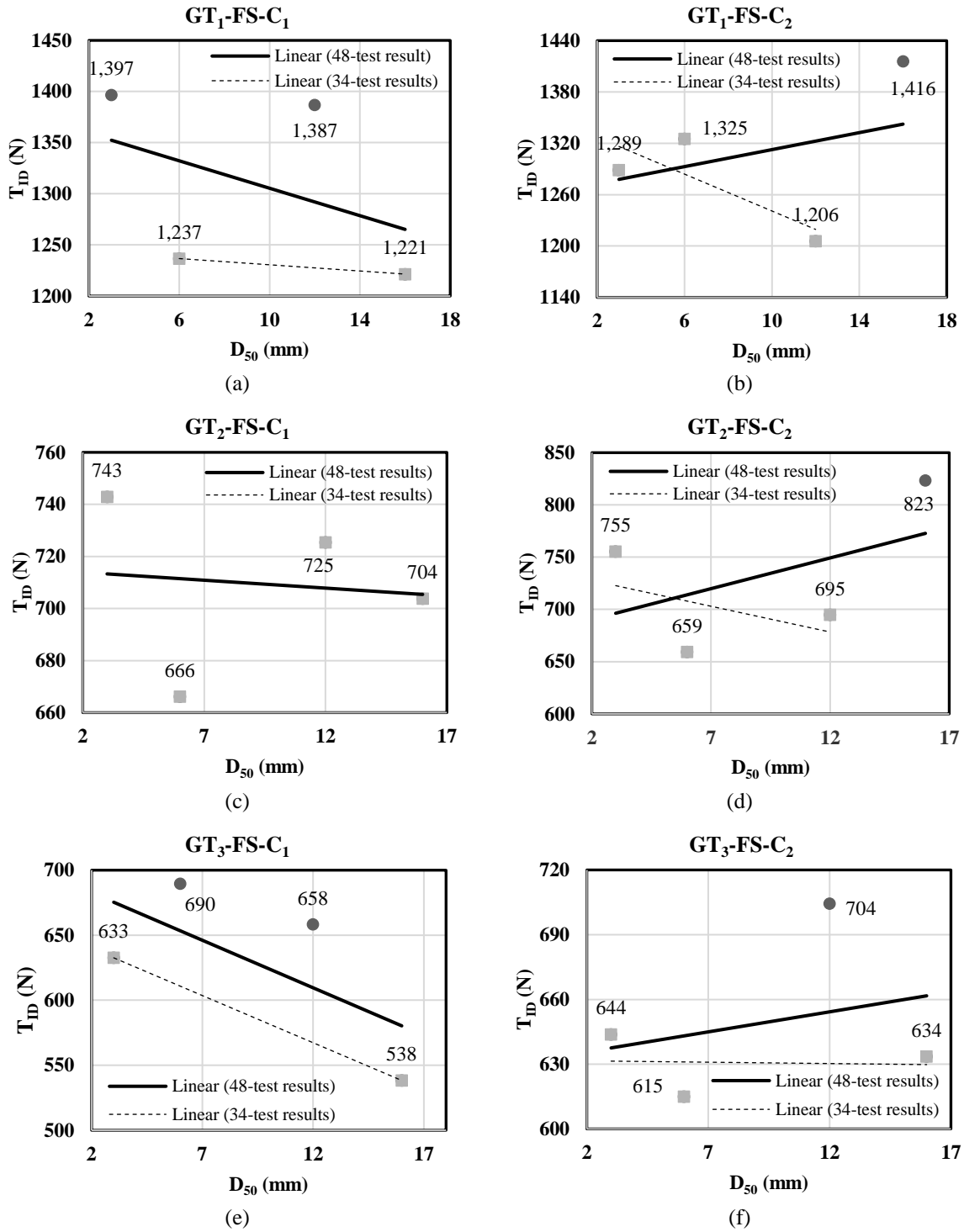


Fig. 6 Retained geotextile tensile strengths for different size backfills all on subgrade "FS". $Dr=70\%$ for (a),

(c) & (e), $D_r = 90\%$ for (b), (d) & (f). Solid lines and dashed lines are plotted with and without considering the "circle points", respectively. These "circle points" represent retained tensile strengths larger than the as-received tensile strengths

316

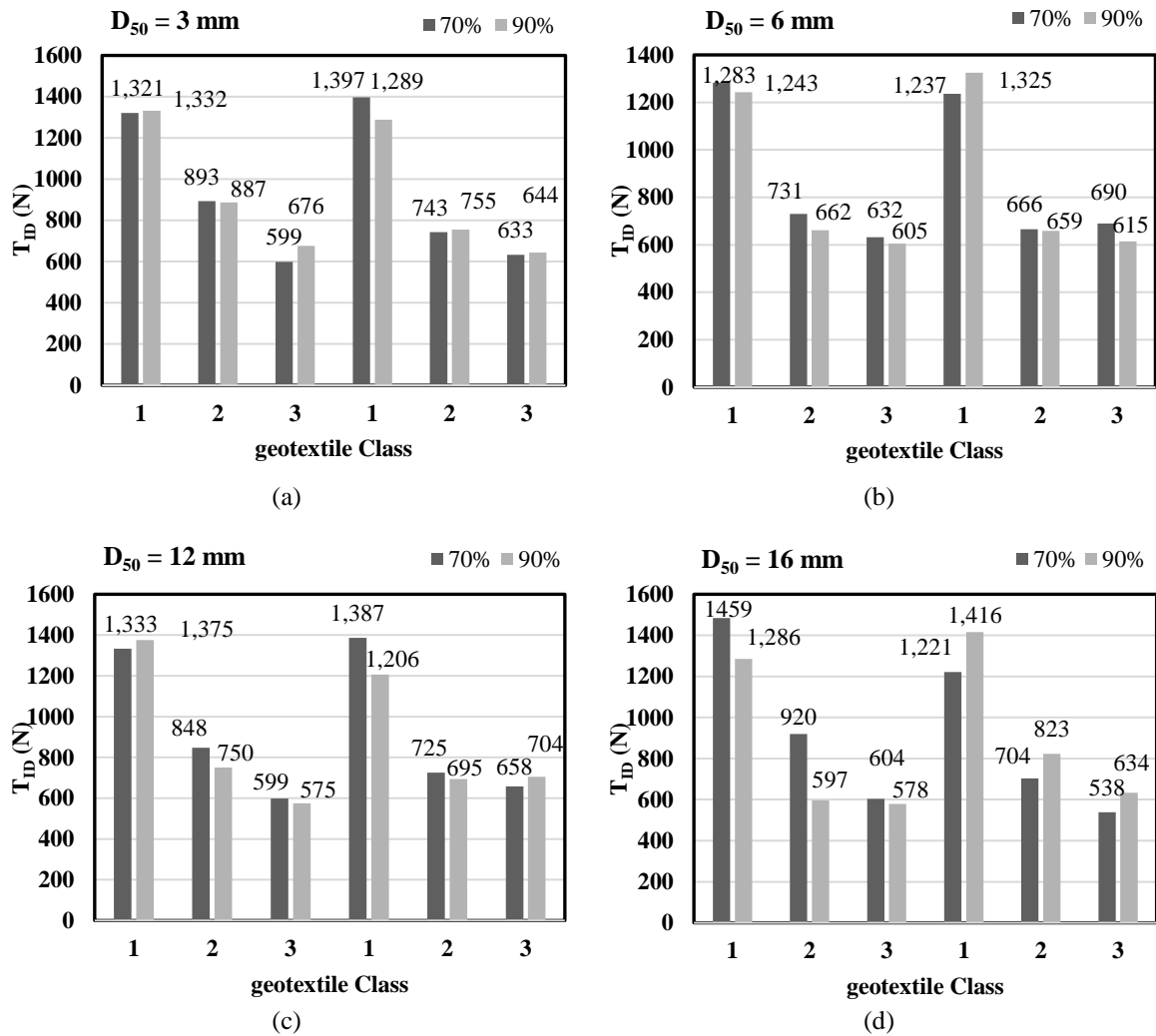


Fig. 7 Variations of retained tensile strength with respect to relative density of the backfill with (a) $D_{50} = 3\text{mm}$, (b) $D_{50} = 6\text{mm}$, (c) $D_{50} = 12\text{mm}$ and (d) $D_{50} = 16\text{mm}$

317

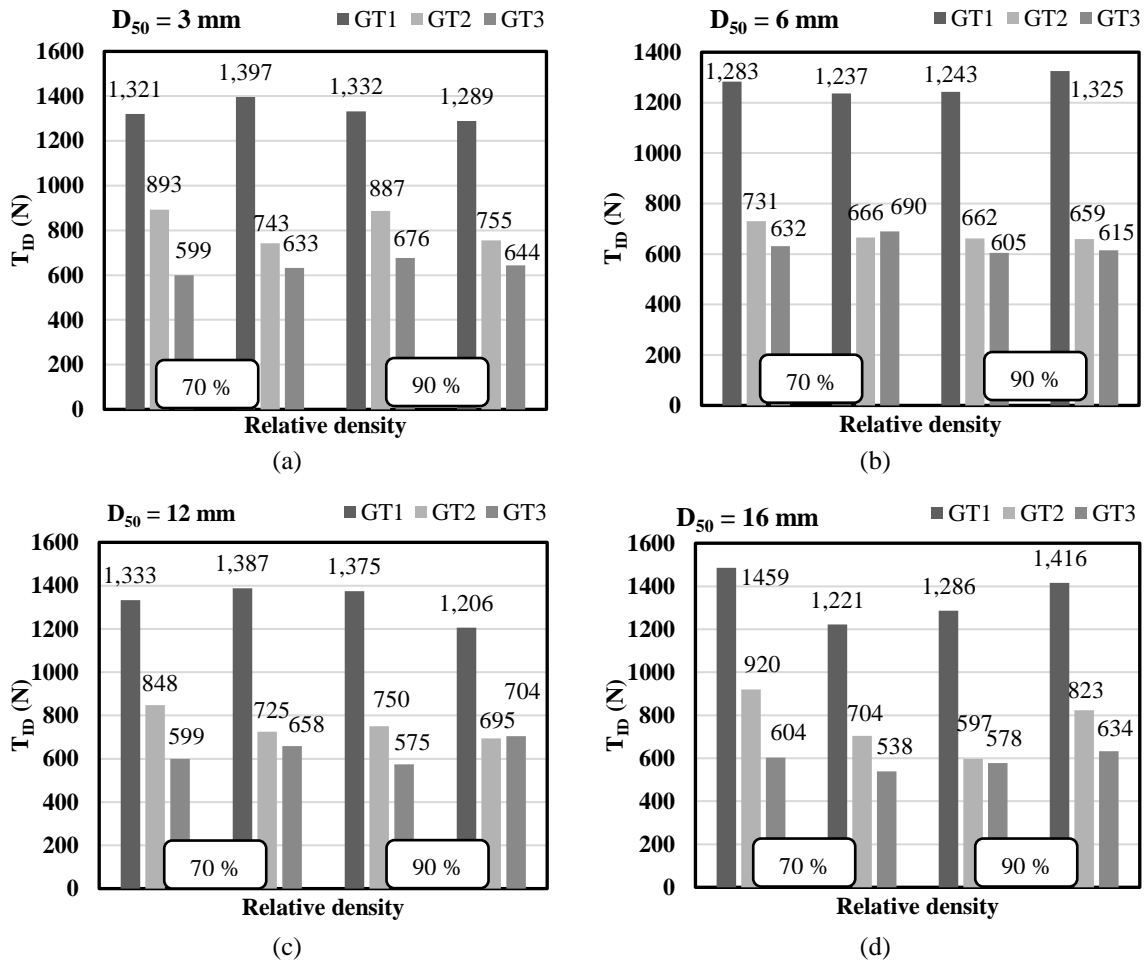


Fig. 8 Variations of retained tensile strength with respect to geotextiles' class for backfill with (a) D_{50} =3mm, (b) D_{50} =6mm, (c) D_{50} =12mm and (d) D_{50} =16mm for the two relative densities shown

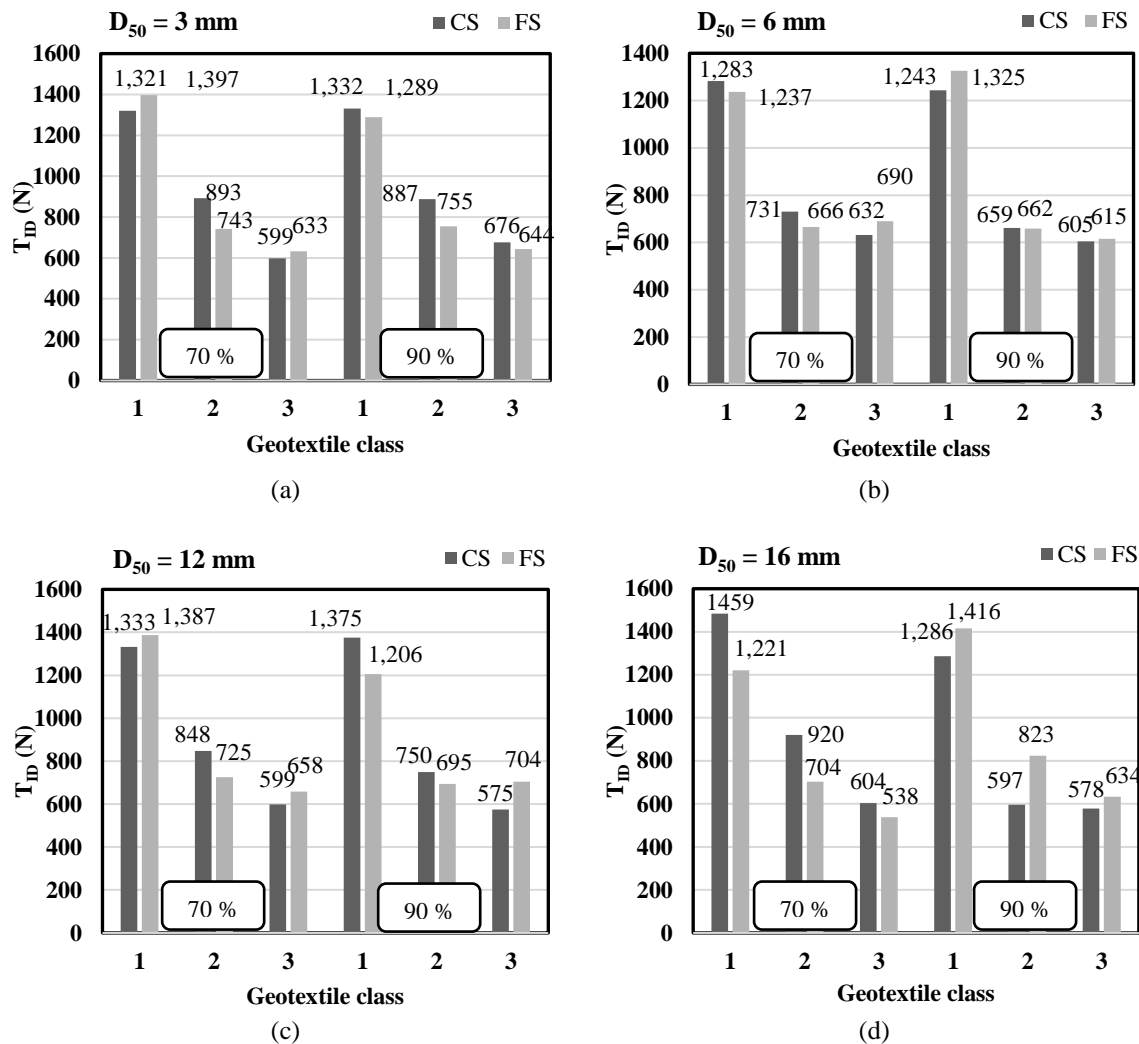


Fig. 9 Variations of retained tensile strength with respect to subgrades' CBR for backfill with (a) $D_{50} = 3$ mm, (b) $D_{50} = 6$ mm, (c) $D_{50} = 12$ mm and (d) $D_{50} = 16$ mm for the two relative densities shown

319

320

321

5.3 Dimensional analysis

322

323

324

325

326

Dimensional analysis aims to generalize our analytical description of a problem based on background knowledge, helping with extrapolation towards the prototype case (Tavakoli Mehrjardi et al. 2016). Eq. (1) lists the major physical parameters influencing the retained tensile strength (T_{ID}):

327

328

329

330

- median grain size of backfill materials (D_{50}) in meters,
- subgrade CBR expressed as a percentage,
- relative density of backfills (D_r) also expressed as a percentage,
- as-received geotextile tensile strength (T_0) in Newtons, and

- 331 • the imposed stress over the geotextiles during installation (σ) in Pascals.
 332 The imposed stresses on the geotextile can be estimated by considering the weight of the soil
 333 above it plus the stress propagated by the compaction energy (for instance based on the Boussinesq
 334 equation).

$$T_{ID} = f(D_{50}, CBR, D_r, T_0, \sigma) \quad (1)$$

335 The equation comprises 5 parameters having two fundamental dimensions (i.e. length and
 336 force). Therefore, Eq. (1) can be reduced to 3 independent parametric groups and arranged non-
 337 dimensionally as in Eq. (2)

$$\frac{T_{ID}}{T_0} = f\left(\frac{T_0}{\sigma D_{50}^2}, D_r, CBR\right) \quad (2)$$

338 Table 8 tabulates these groups for each test. The dimensionless parameter T_{ID} / T_0 is defined as
 339 the ratio of retained strength (S_r) and installation damage reduction factor (RF_{ID}) is thus the
 340 reciprocal of the value (S_r) (see Table 8). Accordingly, reduction factors due to installation of
 341 geotextiles in the backfill were obtained in the range 1~1.34. This range of values is in the line
 342 with that stated in FHWA-NHI-00-044, which suggests $RD_{ID}=1.1\sim 1.4$ for nonwoven geotextiles in
 343 backfill with maximum grain size 20 mm.

344 Since the effects of relative density and subgrade CBR on the retained tensile strength of the
 345 geotextiles were discussed in the previous section, here the remaining parameter in Eq. (3) ($T_0 /$
 346 σD_{50}^2) is analyzed. As can be seen in Fig. 10, an increase of $T_0 / (\sigma D_{50}^2)$ tends to increase the ratio
 347 of retained strength and in turn, reduce the installation damage reduction factor. The implication of
 348 Eq. (2) is that, for a backfill with a grain size 5 times that of some reference size, then the same
 349 damage, in terms of (S_r) and (RF_{ID}), could only be expected if the as-received tensile strength of
 350 the geotextile were 25 times of that in the reference situation. With grain size of the backfill in Eq.
 351 (2) having a power of two, it is clear that damage will be much more sensitive to that than to
 352 normal stress, which has a power of only one.

353

354 5.4 Regression model

355

356 Multiple regression analysis attempts were made to quantify and enumerate Eq. (2) so that it
 357 could be used to estimate the relationships between the variable parameters. The regression model
 358 was evaluated based on coefficient of determination by minimizing the standard error. Several
 359 types of mathematical functions including cubic, quadratic, logarithmic, linear and exponential
 360 functions were considered to select an optimum regression model. Among the possibilities, the
 361 natural-logarithm function was chosen to correlate the ratio of retained tensile strength (S_r), or
 362 installation damage reduction factor (RF_{ID}), with the non-dimensional independent parameters
 363 previously identified CBR, D_r and $T_0 / (\sigma D_{50}^2)$. Eq. (3) and (4) show the empirical relationships
 364 that resulted.

$$R = \frac{T_{ID}}{T_0} = 0 \cdot 875 + 0 \cdot 019 \ln\left(\frac{T_0}{\sigma D_{50}^2}\right) - 0 \cdot 029 \ln(D_r) + 0 \cdot 018 \ln(CBR) \quad (3)$$

$$RF_{ID} = \frac{T_0}{T_{ID}} = 1 \cdot 09 - 0 \cdot 023 \ln\left(\frac{T_0}{\sigma D_{50}^2}\right) + 0 \cdot 046 \ln(D_r) - 0 \cdot 02 \ln(CBR) \quad (4)$$

Table 8 Independent parameters of dimensional analysis based on test conditions

Test code	$T_0/(\sigma D_{50}^2)$	D_r (%)	CBR (%)	S_r	RF_{ID}
GT ₁ -CS-3-C ₁	2158.49	70	49	0.98	1.02
GT ₃ -CS-3-C ₁	1039.27	70	49	0.92	1.09
GT ₂ -FS-3-C ₁	1279.11	70	27	0.93	1.08
GT ₃ -FS-3-C ₁	1039.27	70	27	0.97	1.03
GT ₁ -CS-3-C ₂	2157.88	90	49	0.99	1.01
GT ₁ -FS-3-C ₂	2157.88	90	27	0.95	1.05
GT ₂ -FS-3-C ₂	1278.75	90	27	0.94	1.06
GT ₃ -FS-3-C ₂	1038.98	90	27	0.99	1.01
GT ₁ -CS-6-C ₁	539.28	70	49	0.95	1.05
GT ₂ -CS-6-C ₁	319.57	70	49	0.91	1.10
GT ₃ -CS-6-C ₁	259.65	70	49	0.97	1.03
GT ₁ -FS-6-C ₁	539.28	70	27	0.92	1.09
GT ₂ -FS-6-C ₁	319.57	70	27	0.83	1.20
GT ₁ -CS-6-C ₂	539.14	90	49	0.92	1.09
GT ₂ -CS-6-C ₂	319.49	90	49	0.83	1.21
GT ₃ -CS-6-C ₂	259.59	90	49	0.93	1.07
GT ₁ -FS-6-C ₂	539.14	90	27	0.98	1.02
GT ₂ -FS-6-C ₂	319.49	90	27	0.82	1.21
GT ₃ -FS-6-C ₂	259.59	90	27	0.95	1.06
GT ₁ -CS-12-C ₁	134.87	70	49	0.99	1.01
GT ₃ -CS-12-C ₁	64.94	70	49	0.92	1.09
GT ₂ -FS-12-C ₁	79.92	70	27	0.91	1.10
GT ₂ -CS-12-C ₂	79.90	90	49	0.94	1.07
GT ₃ -CS-12-C ₂	64.92	90	49	0.88	1.13
GT ₁ -FS-12-C ₂	134.84	90	27	0.89	1.12
GT ₂ -FS-12-C ₂	79.90	90	27	0.87	1.15
GT ₃ -CS-16-C ₁	36.53	70	49	0.93	1.08
GT ₁ -FS-16-C ₁	75.87	70	27	0.90	1.11
GT ₂ -FS-16-C ₁	44.96	70	27	0.88	1.14
GT ₃ -FS-16-C ₁	36.53	70	27	0.83	1.21
GT ₁ -CS-16-C ₂	75.85	90	49	0.95	1.05
GT ₂ -CS-16-C ₂	44.95	90	49	0.75	1.34
GT ₃ -CS-16-C ₂	36.52	90	49	0.89	1.12
GT ₃ -FS-16-C ₂	36.52	90	27	0.97	1.03

365
366
367
368
369
370
371
372
373
374
375
376
377
378
379
380
381
382
383
384
385
386
387
388
389
390
391
392
393
394
395
396
397
398
399
400
401
402
403
404

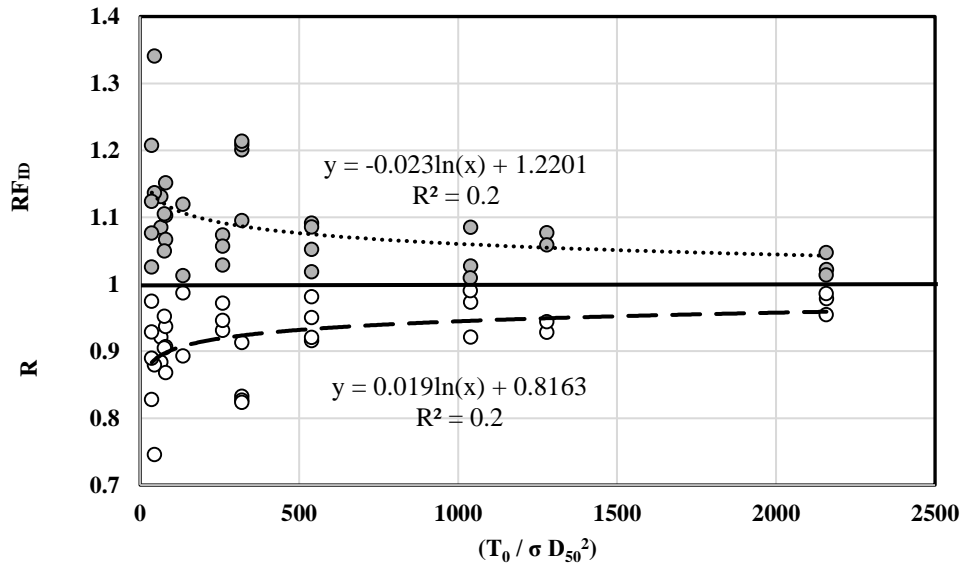


Fig. 10 Effect of the $T_0/(\sigma D_{50}^2)$ on S_r and RF_{ID}

405

406

5.4.1 Validation of the model

407

408

Table 9 shows the values of the statistical parameters for the regression models. Although the coefficient of determinations for both models were about 0.21, the standard errors of the ratio of retained strength (S_r) and of the installation damage reduction factor (RF_{ID}) were 6% and 8%, respectively. This shows that the proposed models with the probabilities of 94% and 92%, are highly representative of the measured results, even though their predictive ability is limited.

412

413

Table 9 Statistical parameters for evaluation of the proposed regression models

414

415

416

417

418

419

To validate the relationships expressed in Eq. (3) and (4), Table 10, containing values of the ratio of retained strength (S_r) and of installation damage reduction factor (RF_{ID}) are presented as obtained by tests results and by the empirical equations. In most of the cases, the values of the residuals (the difference between the predicted and observed values) for the ratio of retained strength (S_r) and for the installation damage reduction factor of geotextiles (RF_{ID}) were around 0.03 and 0.05, respectively. It may be noted that most of the highest residuals belong to geotextile Class 2 with more reliable modelling for Classes 1 & 3.

427

428

5.4.2 Parametric study

429

430

To study the model sensitivity and, also, the predicted values of S_r and RF_{ID} , the effect of different parameters are discussed in the following sections.

431

432

433

Table 10 Comparison of the results obtained by tests and regression models

Test code	Grab tensile test		Eq. (3) and (4)		Residual value	
	S_r	RF_{ID}	S_r	RF_{ID}	S_r	RF_{ID}
GT ₁ -CS-3-C ₁	0.98	1.02	0.97	1.03	0.01	0.01
GT ₃ -CS-3-C ₁	0.92	1.09	0.95	1.05	0.03	0.04
GT ₂ -FS-3-C ₁	0.93	1.08	0.95	1.05	0.02	0.02
GT ₃ -FS-3-C ₁	0.97	1.03	0.94	1.06	0.03	0.03
GT ₁ -CS-3-C ₂	0.99	1.01	0.96	1.04	0.03	0.03
GT ₁ -FS-3-C ₂	0.95	1.05	0.95	1.05	0	0.01
GT ₂ -FS-3-C ₂	0.94	1.06	0.94	1.07	0	0.01
GT ₃ -FS-3-C ₂	0.99	1.01	0.94	1.07	0.05	0.06
GT ₁ -CS-6-C ₁	0.95	1.05	0.94	1.06	0.01	0.01
GT ₂ -CS-6-C ₁	0.91	1.10	0.93	1.08	0.02	0.02
GT ₃ -CS-6-C ₁	0.97	1.03	0.93	1.08	0.04	0.05
GT ₁ -FS-6-C ₁	0.92	1.09	0.93	1.07	0.01	0.02
GT ₂ -FS-6-C ₁	0.83	1.20	0.92	1.09	0.09	0.11
GT ₁ -CS-6-C ₂	0.92	1.09	0.93	1.07	0.01	0.01
GT ₂ -CS-6-C ₂	0.83	1.21	0.92	1.09	0.10	0.12
GT ₃ -CS-6-C ₂	0.93	1.07	0.92	1.09	0.01	0.02
GT ₁ -FS-6-C ₂	0.98	1.02	0.92	1.09	0.06	0.07
GT ₂ -FS-6-C ₂	0.82	1.21	0.91	1.10	0.09	0.12
GT ₃ -FS-6-C ₂	0.95	1.06	0.91	1.10	0.04	0.05
GT ₁ -CS-12-C ₁	0.99	1.01	0.91	1.09	0.07	0.08
GT ₃ -CS-12-C ₁	0.92	1.09	0.90	1.11	0.02	0.03
GT ₂ -FS-12-C ₁	0.91	1.10	0.89	1.12	0.01	0.02
GT ₂ -CS-12-C ₂	0.94	1.07	0.90	1.12	0.04	0.05
GT ₃ -CS-12-C ₂	0.88	1.13	0.89	1.12	0.01	0.01
GT ₁ -FS-12-C ₂	0.89	1.12	0.90	1.12	0	0
GT ₂ -FS-12-C ₂	0.87	1.15	0.89	1.13	0.02	0.02
GT ₃ -CS-16-C ₁	0.93	1.08	0.89	1.12	0.04	0.05
GT ₁ -FS-16-C ₁	0.90	1.11	0.89	1.12	0.01	0.01
GT ₂ -FS-16-C ₁	0.88	1.14	0.88	1.13	0	0.01
GT ₃ -FS-16-C ₁	0.83	1.21	0.88	1.14	0.05	0.07
GT ₁ -CS-16-C ₂	0.95	1.05	0.90	1.12	0.06	0.07
GT ₂ -CS-16-C ₂	0.75	1.34	0.89	1.13	0.14	0.21
GT ₃ -CS-16-C ₂	0.89	1.12	0.88	1.14	0.01	0.01
GT ₃ -FS-16-C ₂	0.97	1.03	0.87	1.15	0.10	0.12

434

435

a) Effect of as-received grab tensile strength (T_0)

436

437

438

439

440

441

442

Fig. 11 illustrates the effect of as-received grab tensile strength of the geotextiles on the ratio of retained strength (S_r) and installation damage reduction factor of geotextiles (RF_{ID}) as estimated using Eq. (3) and (4). The values of σ , D_{50} , D_r and CBR remain constant, equal to 100 kPa, 12 mm, 100% and 80%, respectively. According to Fig. 11, it can be found out that selection of geotextiles with higher as-received grab tensile strength results in lower installation damage.

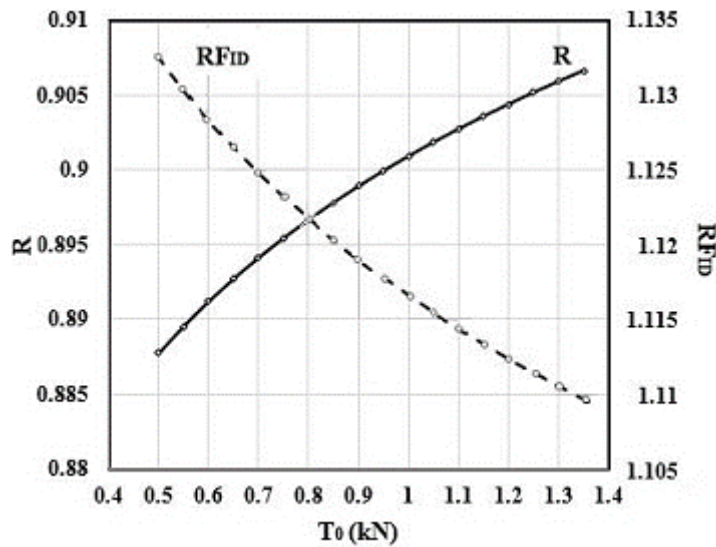


Fig. 11 Effect of as-received grab tensile strength of the geotextiles (T_0) on geotextiles' survivability

443

444

b) Effect of transferred stress at the level of geotextile (σ)

445

446

447

448

449

450

451

452

453

As mentioned before, the transferred stress at the level of geotextile can be the result of the backfill's weight and of the stress propagated by the compactor energy, and having a direct role in the installation damage. Fig. 12 is presented to illustrate the effect of applied stress on geotextiles' installation damage in which $T_0 = 650$ N, $D_{50} = 12$ mm, $D_r = 70\%$ and $CBR = 80\%$, using Eq. (3) and (4). The results show the damage of geotextiles consequent on the transferred stress intensification. Therefore, as may have been anticipated, lighter compactors and thicker cover of the backfill materials over the geotextile should be utilized, as much as possible.

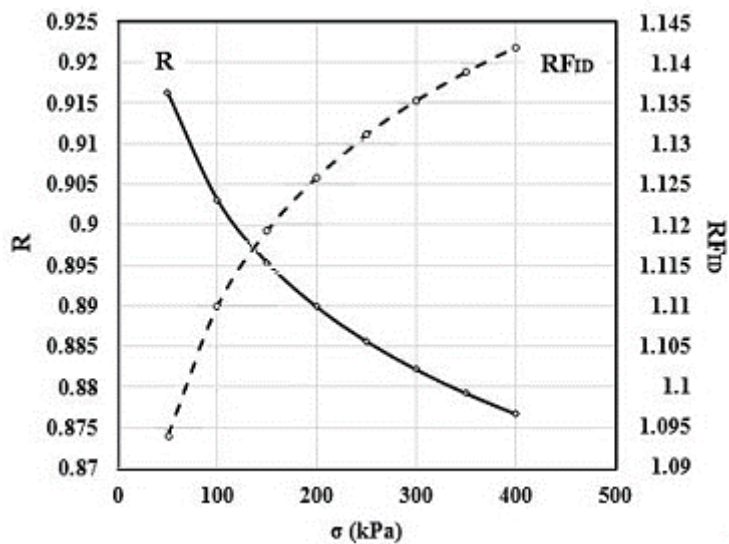


Fig. 12 Effect of transferred stress level (σ) on geotextiles' survivability

454
455
456
457
458
459
460
461
462
463
464

c) Effect of backfill's median grain size (D_{50})

The test results revealed that the median grain size of the backfill highly affected the retained tensile strength of the geotextiles. Fig. 13 relates the median grain size to the ratio of retained strength (S_r) and installation damage reduction factor of geotextiles (RF_{ID}). The values of T_0 , σ , D_r and CBR are fixed as 650 N, 100 kPa, 70% and 80%, respectively. As can be seen, increasing the soil particle size intensifies the installation damage of the geotextiles. Therefore, using high-survivability geotextiles (i.e. class 1 per AASHTO M288-08) in backfills that contain large particle sizes is highly recommended.

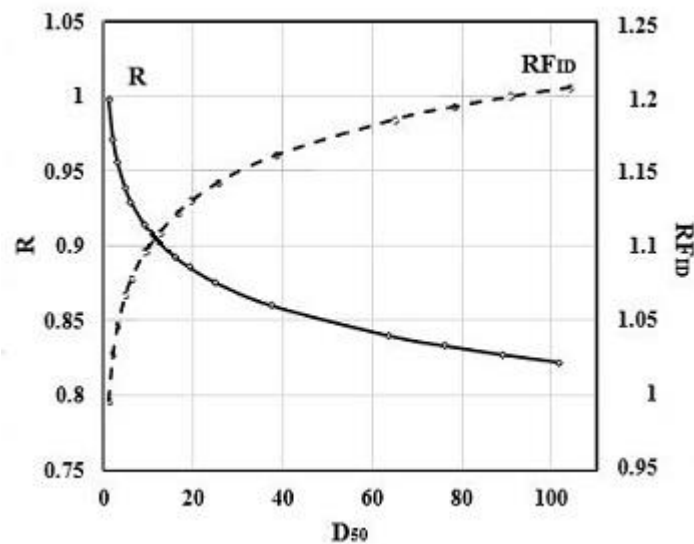


Fig. 13 Effect of backfill's median grain size (D_{50}) on geotextiles' survivability

465
466
467
468
469
470
471
472
473
474
475
476

d) Effect of backfill's relative density (D_r)

In order to study the impact of the backfill's relative density on the ratio of retained strength and installation damage of the geotextiles, Fig. 14 is plotted. To assess only this parameter requires that the values of T_0 , D_{50} , CBR and σ remaining constant, selected here as 650 N, 12 mm, 80% and 100 kPa, respectively. According to Figs. 12 and 14, it can be concluded that the variation of installation damage reduction factor due to transferred stress and due to relative density are of the same order.

e) Effect of subgrades' CBR

477
478
479
480
481

Conceivably, the subgrades' CBR is effective in controlling installation damage of geotextiles due to its direct effect on the amount of extension in a geotextile layer that is under imposed stress. Fig. 15, in which $T_0 = 650$ N, $D_{50} = 12$ mm, $D_r = 70\%$ and $\sigma = 100$ kPa, shows how much the bearing capacity of the subgrades can influence the survivability of the geotextiles from installation damage. The results confirm the continued weakness of geotextiles that are placed on weaker

482 subgrades. FHWA HI-95-038 recommends that higher survivability geotextiles should be used
 483 when the subgrade has low shear strength.
 484
 485

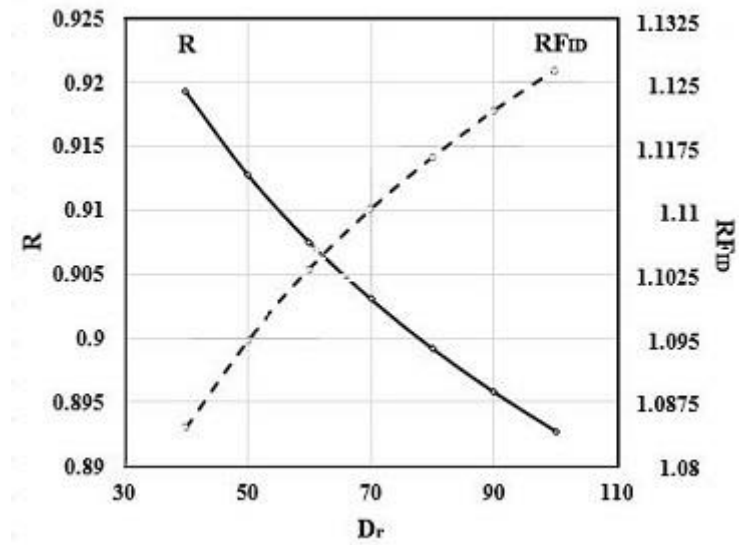


Fig. 14 Effect of backfill's relative density (D_r) on geotextiles' survivability

486

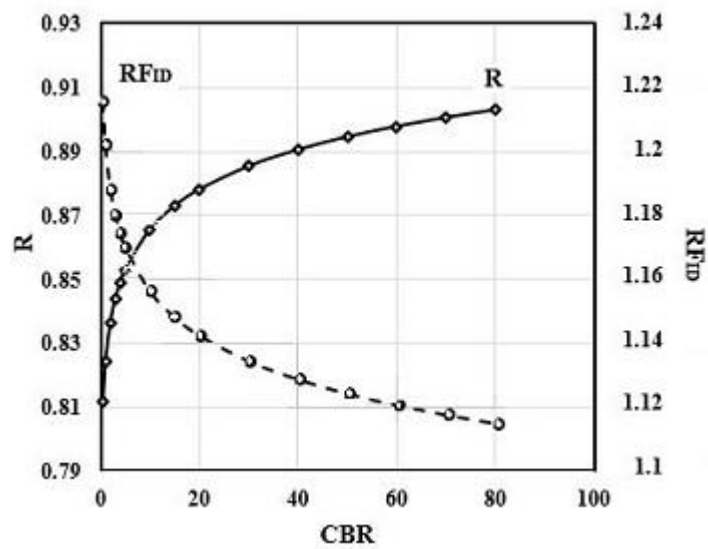


Fig. 15 Effect of subgrade' CBR on geotextiles' survivability

487
 488
 489

6. Summary and conclusion

Because the performance and survivability of geotextiles has a major effect on the economy of design, understanding and quantifying this is crucially important, and increasingly so as soil reinforcement technology because more and more prevalent. Therefore, the survivability of geotextiles should be verified by conducting tests under field conditions, especially for major projects. In the study reported in this paper, to assess installation damage at full-scale, a field test was employed to simulate unpaved road construction. Together with laboratory tests, this quantified the retained tensile strength of some geotextiles. Various parameters were investigated (four specially poor-graded fill materials, two kinds of subgrades with different CBR, three nonwoven needle-punched geotextiles with Classes 1, 2 and 3 (according to AASHTO M288-08) and two different relative densities for backfill materials). The results of the study, as applied to geotextile installations, can be summarized as follows:

- Neither fraying, fiber separation nor holes were observed. However, in all specimens, fine-grained particles were found to have entered into the texture of the geotextiles. Also, backfills with a median grain size of 12 and 16 mm, squeezed into the geotextiles' texture, especially in Class 2 and 3 types.
- The proposed models for predicting the ratio of retained tensile strength (S_r) and installation damage reduction factor (RF_{ID}) are highly representative of the measured results, even though their predictive ability is limited.
- The retained tensile strength of the geotextiles was significantly reduced as the median grain size (D_{50}) of the backfill increased.
- Tensile strengths of the geotextile decreased following placement of compacted fill to a high relative density. The greater compaction stress passed down to the geotextile, resulted in a greater reduction in the retained tensile strength.
- Selection of geotextiles with higher as-received grab tensile strength (increasing the geotextiles Class from 3 to 1) results in reduced installation damage.
- The subgrades' CBR is implicated in the amount of installation damage of geotextiles, probably due to its direct effect on the amount of extension in the geotextile layer caused by the imposed stress.
- The Dimensionless parameter of $T_0 / (\sigma D_{50}^2)$ implies that the change of geotextile damage will be more sensitive to change in median grain size of the backfill, with a power of two, as compared to changes in transferred stress, with a power of one.

This study investigated tensile strength reduction factors of nonwoven geotextiles for reinforcement and stabilization applications on low shear strength subgrades. Since, the obtained results are unlikely to be applicable to woven geotextiles, investigations on that material are highly recommended.

529 **References**

530

531 AASHTO M288-08 (2008), Standard Specification for Geotextile Specification for Highway Applications,
532 American Association of State Highway and Transportation Officials, Virginia, USA.533 Allen, T.M. and Bathurst, R.J. (1994), "Characterization of geosynthetic load-strain behavior after
534 installation damage", *Geosynthetics International* 1(2), 181-199.535 ASTM D 1556-08 (2008), Standard Test Method for Density and Unit Weight of Soil in Place by Sand-Cone
536 Method, American Society for Testing and Materials, West Conshohocken, PA, USA.537 ASTM D 5261-10 (2010), Standard Test Method for Measuring Mass per Unit Area of Geotextiles,
538 American Society for Testing and Materials, West Conshohocken, PA, USA.539 ASTM D 5821-13 (2013), Standard Test Method for Determining the Percentage of Fractured Particles in
540 Coarse Aggregate, American Society for Testing and Materials, West Conshohocken, PA, USA.541 ASTM D 6241-14 (2014), Standard Test Method for Static Puncture Strength of Geotextiles and Geotextile-
542 Related Products Using a 50-mm Probe, American Society for Testing and Materials, West
543 Conshohocken, PA, USA.544 ASTM D4533-15 (2015), Standard Test Method for Trapezoidal Tearing strength of Geotextiles,
545 American Society for Testing and Materials, West Conshohocken, PA, USA.546 ASTM D4632-15 (2015), Standard Test Method for Grab Breaking Load and Elongation of Geotextiles,
547 American Society for Testing and Materials, West Conshohocken, PA, USA.548 ASTM D5818 (2000), Obtaining Samples of Geosynthetics from a Test Section for Assessment of
549 Installation Damage, American Society for Testing and Materials, West Conshohocken, PA, USA.550 Bathurst, R.J., Huang, B. and Allen, T.M. (2011), Analysis of installation damage tests for LRFD calibration
551 of reinforced soil structures, *Geotextiles and Geomembranes*, **29**(3), 323-334.552 Berg, R.R, Christopher, B.R. and Samtani, N.C. (2009), Design of mechanically stabilized earth walls and
553 reinforced soil slopes – Vol. (1) FHWA NHI-10-024, Federal Highway Administration, Washington.554 Carlos, D.M., Pinho-Lopes, M., Carneiro, J.R. and Lopes, M.L. (2015), "Effect of soil grain size distribution
555 on the mechanical damage of nonwoven geotextiles under repeated loading", *International Journal of*
556 *Geosynthetics and Ground Engineering*, 1-9.557 Costa, C.M.L., Zornberg, J.G., Boeno, B.D.C. and Costa, Y.D.J. (2016), "Centrifuge evaluation of the time-
558 dependent behavior of geotextile-reinforced soil walls", *Geotextiles and Geomembranes*, **44**(2), 188-
559 200.560 Deb, K. and Konai, S. (2014), "Bearing capacity of geotextile-reinforced sand with varying fine fraction",
561 *Geomechanics and Engineering*, **6**(1), 33-45.562 Elias, V. (2001), "Corrosion/degradation of soil reinforcements for mechanically stabilized earth walls and
563 reinforced soil slopes", FHWA-NHI-00-044, Federal Highway Administration, Washington.564 Elvidge, C.B. and Raymond, G.P. (1999), "Laboratory survivability of nonwoven geotextiles on open-
565 graded crushed aggregate", *Geosynthetics International*, **6**(2), 93-117.566 FHWA-HI-95-038 (1998), Geosynthetic design and construction guidelines, Federal Highway
567 Administration, Washington, USA.568 Greenwood, J.H. and Brady, K.C. (1992), "Geotextiles in aggressive soils", *Construction and Building*
569 *Materials*, **6**(1), 15-18.570 Hosseinpour, I., Almeida, M.S.S. and Riccio, M. (2015), "Full-scale load test and finite-element analysis of
571 soft ground improved by geotextile-encased granular columns", *Geosynthetics International*, **22**(6),
572 428-438.573 Hufenus, R., Rügger, R., Flum, D. and Sterba, I.J. (2005), "Strength reduction factors due to installation
574 damage of reinforcing geosynthetics", *Geotextiles and Geomembranes*, **23**(5), 401-424.575 Kim, H.J., Won, M.S., Lee, J.B., Joo, J.H. and Jamin, J.C. (2015), "Comparative study on the behavior of
576 soil fills on rigid acrylic and flexible geotextile containers", *Geomechanics and Engineering*, **9**(2), 243-
577 259.

- 578 Koerner, G.R. and Koerner, R.M. (1990), "The installation survivability of geotextiles and geogrids", *Fourth*
579 *International Conference on Geotextiles, Geomembranes and Related Products*, Den Haag, 597–602.
- 580 Mendes, M.J.A., Palmeira, E.M. and Matheus, E. (2007), "Some factors affecting the in-soil load–strain
581 behaviour of virgin and damaged nonwoven geotextiles", *Geosynthetics International* **14**(1), 39-50.
- 582 Naeini, S.A. and Gholampoor, N. (2014), "Cyclic behaviour of dry silty sand reinforced with a geotextile",
583 *Geotextiles and Geomembranes*, **42**(6), 611-619.
- 584 Nikbakht, M. and Diederich, R. (2008), "The energy potential and its integration in the national European
585 specification", *Foundations of Civil and Environmental Engineering*, 41-53.
- 586 Pinho-Lopes, M. and Lopes, M.L. (2013), "Tensile properties of geosynthetics after installation damage",
587 *Environmental Geotechnics*, **1**(3), 161-178.
- 588 Portelinha, F.H.M., Bueno, B.S. and Zornberg, J.G. (2013), "Performance of nonwoven geotextile-reinforced
589 walls under wetting conditions: laboratory and field investigations", *Geosynthetics International*, **20**(2),
590 90-104.
- 591 Portelinha, F.H.M., Zornberg, J.G. and Pimentel, V. (2014), "Field performance of retaining walls reinforced
592 with woven and nonwoven geotextiles", *Geosynthetics International*, **21**(4), 270-284.
- 593 Richardson, G.N. (1998), "Field evaluation of geosynthetic survivability in aggregate road base",
594 *Geotechnical Fabrics Report*, 34-38.
- 595 Rosete, A., Lopes, P.M., Pinho-Lopes, M. and Lopes, M.L. (2013), "Tensile and hydraulic properties of
596 geosynthetics after mechanical damage and abrasion laboratory tests", *Geosynthetics International*, **20**
597 (5), 358-374.
- 598 Tandel, K.Y., Solanki, C.H. and Desai A.K. (2014), "Field behaviour geotextile reinforced sand column",
599 *Geomechanics and Engineering*, **6**(2), 195-211.
- 600 Tavakoli Mehrjardi, Gh. and Amjadi Sardehaei, E., (2017). "Design graphs to estimate reduction factor of
601 nonwoven geotextiles due to installation process" *European Journal of Environmental and Civil*
602 *Engineering*, DOI: 10.1080/19648189.2017.1327897, 1-14.
- 603 Tavakoli Mehrjardi, Gh., Ghanbari, A. and Mehdizadeh, H. (2016), "Experimental study on the behaviour of
604 geogrid-reinforced slopes with respect to aggregate size", *Geotextiles and Geomembranes*, **44**(6), 862-
605 871.
- 606 Tavakoli Mehrjardi, Gh., Moghaddas Tafreshi, S.N. and Dawson, A. R. (2013), "Pipe response in a geocell
607 reinforced trench and compaction considerations", *Geosynthetics International*, **20**(2), 105-118.
- 608 Vieira, C.S., Lopes, M.D.L. and Caldeira, L. (2015), "Sand-Nonwoven geotextile interfaces shear strength
609 by direct shear and simple shear tests", *Geomechanics and Engineering*, **9**(5), 601-618.
- 610 Vieira, C.S. and Pereira, P.M. (2015). "Damage induced by recycled Construction and Demolition Wastes
611 on the short-term tensile behaviour of two geosynthetics", *Transportation Geotechnics*, **4**(September),
612 64-75.
- 613 Wang, L., Zhang, G. and Zhang, J.M. (2011), "Centrifuge model tests of geotextile-reinforced soil
614 embankments during an earthquake", *Geotextiles and Geomembranes*, **29**(3), 222-232.
- 615 Watn, A., Eiksund, G. and Knutson, A. (1998), "Deformation and damage of nonwoven geotextiles in road
616 construction", *Sixth International Conference on Geosynthetics*, 933-938.
- 617 Watts, G.R.A. and Brady, K.C. (1994), "Geosynthetics-installation damage and the measurement of tensile
618 strength", *Fifth International Conference on Geotextiles, Geomembranes and Related Products*,
619 Singapore, 1159–1164.
- 620 WSDOT T925 (2005), "Standard Practice for Determination of Long-Term Strength for Geosynthetic
621 Reinforcement", Washington State Department of Transportation, Olympia, Washington, USA.
- 622
- 623
- 624
- 625
- 626

627

Nomenclature		
Symbol	Units	Meaning
C_u	-	Coefficient of uniformity
C_c	-	Coefficient of curvature
CBR	(%)	Subgrade CBR
CS	-	Coarse-grained subgrade
D_r	(%)	Backfill's relative density
D_{10}	(mm)	Effective grain size
D_{30}	(mm)	Grain size of 30% passing percentage
D_{50}	(mm)	Median grain size
D_{60}	(mm)	Grain size of 60% passing percentage
FS	-	Fine-grained subgrade
G_s	-	Specific gravity of soil
R^2		Coefficient of Regression
RF_{ID}		Installation damage reduction factor of geotextile
S_r		Ratio of retained strength of geotextile
σ	(Pa)	Transferred stress at the level of geotextile
T_0	(N)	As-received Grab tensile strength of the geotextiles
T_{ID}	(N)	Retained Grab tensile strength of the geotextiles
$T_0 / (\sigma D_{50}^2)$	-	Characteristic parameter

628